Egypt. J. Chem. **Vol. 65**, No. 9 pp. 281 – 291 (2022)

Egyptian Journal of Chemistry

http://ejchem.journals.ekb.eg/

New ligand metal complexes: synthesis, spectroscopic, DFT, and docking studies, and molecular structure

Ehab M Zayed

Department of Green Chemistry, National Research Centre (NRC), 33 EL-Bohouth Street (former EL-Tahrir Street), Dokki Giza Egypt, P.O.12622

Abstract

Analytical techniques, spectrum (IR and ^{1}H NMR), molar conductivity, and magnetic moment measurements were used to synthesize and analyze a ligand (H2L) and its complexes. The thermal analysis (TG) technique was investigated at temperatures ranging from ambient temperature to 1000 degrees Celsius. The ligand (H2L) coupled to the metal ions through two nitrogen and two oxygen atoms in a negative mode, according to the IR spectra. The energy gaps and other critical theoretical parameters were estimated using the DFT/B3LYP method, and the structural formula of the synthesized ligand was optimized using the Gaussian09 program. The agar diffusion method was used to screen the in vitro biological activity of the ligand (H2L) and its metal complexes against Gram(+) bacteria (Bacillis subtilis and Staphylococcus aureus) and Gram(-) bacteria (Escherichia coli and Pseudomonas aeruginosa). The results showed that the produced complexes were more physiologically active than the ligand. A molecular docking research was conducted between the ligand and the crystal structures of 3t88-Escherichia coli, 3ty7-Staphylococcus aureus, 5h67-Bacillus subtilis, and 5i39-Pseudomonas aeruginosa.

Keywords: ligand complexes, spectroscopic and thermal analyses, antimicrobial activity, anticancer activity, Molecular docking

1. Introduction

Many cyclic peptides are employed in medicine, and the majority of them are derived from natural cyclic peptides. Because cyclic peptides have various properties that make them appealing as lead compounds for drug development and useful instruments for biochemical study, scientists have made a variety of efforts to generate physiologically active cyclic peptide molecules [1-5]. As a result, synthetic peptides can be used as early biological leads to quickly identify the molecular structural requirements of active pharmacological modulators. Many natural and synthetic peptides with interesting biological functions are being described on a regular basis.[6-11] Synthetically, active linear peptides can be converted into their cyclic congeners, or peptidomimetics, by attaching one end of the peptide to the other with an amide bond between the amino and carboxyl termini N-to-C (or head-to-tail). Due to their ability to bind and transport metal ions, macrocyclic peptide ligands with additional donor atoms attached to the ring have piqued interest. The synthesis of macrocyclic compounds continues to pique people's interest. Because of their prospective uses in fundamental and applied sciences [12, 13], as well as their anticancer activity and importance in the field of coordination chemistry, they have a tremendous impact on cancer treatment.[14, 15] Certain metal ions bind to cyclic peptides with a high degree of selectivity. Studies have demonstrated that cyclopeptides like vasopressin and oxytocin, which appear to be naturally metal-free, can successfully bind metal ions.[16, 17] Peptide bonds were formed between the N-terminal amine and the C-terminal carboxylate groups of linear precursors to produce cyclic peptides. In His-containing peptides, the N-terminal amino group (also known as the metal ion anchoring group) has an effect on complex formation.[18-20]. Cd(II), Mn(II), and Zn(II) complexes of a newly synthesized cyclopeptide ligand were produced and studied utilizing various analytical and physicochemical techniques in this paper. Their antibacterial activity was tested against a variety of bacterium organisms. To get an understanding of the possible mechanistic action in the search for good potent ant tubercular candidates, molecular docking experiments were done against the crystal structures of 3t88-Escherichia coli, 3ty7-

*Corresponding author e-mail: ehab_zayed2002@yahoo.com
Received date 19 December 2021; revised date 27 January 2022; accepted date 07 February 2022
DOI: 10.21608/EJCHEM.2022.111936.5087
©2022 National Information and Documentation Center (NIDOC)

Staphylococcus aureus, 5h67-Bacillus subtilis, and 5i39-Pseudomonas aeruginosa.

2. Experimental

2. l. Materials and reagents:

All chemicals used were of the analytical reagent grade (AR), and of highest purity available. The chemicals used involved were supplied from Sigma-Aldrich. $MnCl_2.2H_2O$ (BDH), $CuCl_2.2H_2O$ (BDH) and $CdCl_2.2H_2O$ (BDH) (Prolabo) were used. Organic solvents were spectroscopic pure from BDH included ethanol, diethyl ether and dimethylformamide. Hydrogen peroxide, sodium chloride, sodium carbonate, glacial acetic acid and sodium hydroxide (A.R.) were used.

2.2. Solutions

For molar conductivity measurement, $1x10^{-3}$ M stock solutions of the ligand and metal complexes were prepared using dimethylformamide solvent. For measuring UV–Vis absorption spectra, $1x10^{-4}$ M solutions of the ligand and metal complexes were prepared by accurate dilution from the previous prepared stock solutions. For the preparation of RPMI-l640 medium, sodium bicarbonate (Sigma Chemical Co., St. Louis, Mo, USA) was used. In normal saline, 0.05% isotonic Trypan blue solution (Sigma Chemical Co., St. Louis, Mo, USA) was prepared and used to count viability. Sigma Chemical Co., St. Louis, Mo, USA supplied 10 percent Fetal Bovine Serum (FBS) (heat inactivated at 56 ^oC for 30 min), l00 units/ml Penicillin and 2 mg/ml Streptomycin were used prior to use for RPMI-1640 medium supplementation. For cell harvesting, 0.025 percent (w/v) Trypsin (Sigma Chemical Co., St. Louis, Mo, USA) was used. For the dissolution of the unbound SRB dye, 1% (v/v) Acetic acid (Sigma Chemical Co., St. Louis, Mo, USA) was used. As a protein dye, 0.4% of Sulphorhodamine-B (SRB) (Sigma Chemical Co., St. Louis, Mo, USA) dissolved in 1% acetic acid was used. A stock solution (TCA, 50%, Sigma Chemical Co., St. Louis, Mo, USA) of trichloroacetic acid has been prepared and processed. To yield a final concentration of 10 percent used for protein precipitation, 50 µL of the stock was applied to 200 µl RPMI-l640 medium/well. Isopropanol 100 percent and ethanol 70 percent were used. For SRB dye solubilization, Tris base 10 mM (pH 10.5) was used. In 1000 ml of distilled water, 121.1 g of tris base was dissolved and pH was modified by HCl acid (2 M).

2.3. Instrumentations

Carbon, hydrogen and nitrogen microanalyses were performed using the CHNS-932 (LECO) Vario Elemental Analyzer at the Microanalytical Center, Cairo University, Egypt. FT-IR spectra were registered as KBr discs. At room temperature, electronic spectra were registered as solutions in ethanol on a Shimadzu 3101pc spectrophotometer. As a solution in DMSO-d_6, ^1H NMR spectra were recorded at room temperature on a 500 MHz Varian-Oxford Mercury using TMS as an internal standard. Using the Jenway 4010 conductivity meter, the molar conductivity of 10-3 M solid complex solutions in DMF was calculated. The absorption spectra were recorded for 1×10^{-4} M solutions of the free ligand and metal complexes. The spectra were scanned within the wavelength range from 200 to 700 nm. Thermogravimetric analyses (TG and DTG) of solid complexes were performed using the Shimadzu TG-50H thermal analyzer from room temperature to 1000 ^oC. A (Quanta FEG250) SEM, National Research Centre, Egypt) recorded a scanning electron microscope (SEM) image of the complexes. Using the MS-5988 GS-MS Hewlett-Packard instrument at the Microanalytical Center, National Research Centre, Mass spectra were recorded by the EI technique at 70 eV. The antimicrobial activities were carried out at Cairo University, Microanalytical Centre**.**

2.4. Synthesis of ligand

N1,N3-bis(1-hydrazinyl-1-oxopropan-2-yl)isophthalamide: Yield: 65; m.p. 269–271 0C. Rf x100 (solvent system) 35 (S). [α]25D: - 112.00 (C, 0.02, DMSO). IR in (cm−1; KBr): 3050 (NH-stretching), 3100 (CH-arom), 2900 (CH-aliphatic.), 1643 (C=O, hydrazide), 1610 and 1740 (C=O- amide I+ II). ^1H-NMR (500 MHz, DMSO-d6) δ: 8.75 (s, 2H, CONHNH2, D2O exchangeable), 8.40, 8.34 (s, 2H, CONHCH, D2O exchangeable), 8.02–7.52 (s, 4H, aromatic H),4.49–4.47 (q, 2H, CHNH), 4.19 (s, 4H, CONHNH2), 3.66 (s, 6H, OCH3, disappeared), 1.35, 1.33 (d, 6H, 2CH3, CHCH3). ^{13}C-NMR (125 MHz, δ, ppm, DMSO-*d6*): 172.27 (2C, CO, hydrazide), 166.27 (2C, CONH), 165.00 (2C, isophthaloyl, C1, 5), 134.51 (2C, isophthaloyl, C2, 4),130.78 (1C, isophthaloyl, C3),128.67 (1C, isophthaloyl, C6), 52.35 (2C, OCH3, L-ala, disappeared), 48.74 (2C, CHCH3), 17.33, 17.25 (2C, CHCH3). MS (EI, 70 eV): m/z (%) =337 (M++1, 1.65%), 336 (M+, 0.76%), 273 (100%), 76 (29.37%), 50 (7.46%). Molecular formula (M.wt.), C16H20N2O6 (336.3), calculated analysis; C, 57.14; H, 5.99; N, 8.33, found; C 57.11, H 5.90, N 8.31.

2.5. Synthesis of metal complexes

By mixing equal amounts (0.892mmol) of hot saturated ethanol solution of the ligand with the same metal chloride ratio, the Mn(II), Cd(II) and Cu(II) complexes were prepared (lM : lL molar ratio). For three hours, the mixture was refluxed. Through

filtration, the resulting precipitates were collected and washed several times with hot ethanol until the filtrates become clear. In order to provide 88, 88 and 86 percent yield of Cu(II), Cd(II) and Mn(II) complexes, respectively. The solid complexes then dried in desiccator over anhydrous calcium chloride.

N1,N3-bis(1-hydrazinyl-1-oxopropan-2-yl)isophthalamide Cu(II) chloride $[Cu(H_2L)(H_2O)_2].Cl_2$; Yield 88%; m.p. 279 °C; DarkBlue solid. Anal. Calc. for $C_{14}H_{24}Cl_2CuN_6O_6$ (%): C, 33.18; H, 4.77; N, 16.58; M, 12.54. Found (%):C, 33.14; H, 4.70; N, 16.52; M, 12.49. FT-IR (KBr, ν, cm^{-1}) 3073(NH stretching), 2936 (CH, aromatic), 2094 (CH aliphatic) and 1767 (CONH), 1555 (NH2), 532 (M─O), 430 (M─N). μ_{eff} (BM) 1.84; Λ_m (Ω^{-1} mol^{-1} cm^2) 115. UV-Vis (λ_{max}, nm): 270 (π–π* of aromatic rings).

N1,N3-bis(1-hydrazinyl-1-oxopropan-2-yl)isophthalamide Cd(II) chloride $[Cd(H_2L)(H_2O)_2].Cl_2$; Yield 88%; m.p. 281 °C; White green solid. Anal. Calc. for $C_{14}H_{24}Cl_2CdN_6O_6$ (%): C, 30.26; H, 4.35; N, 15.12 ; M, 20.23. Found (%): C, 30.21; H, 4.29; N, 15.07; M, 20.19. FT-IR (KBr, ν, cm^{-1}) 3075(NH stretching), 2936 (CH, aromatic), 2094 (CH aliphatic) and 1770 (CONH), 1558 (NH2), 537 (M─O), 434 (M─N). μ_{eff} (BM) diamagnetic; Λ_m (Ω^{-1} mol^{-1} cm^2) 75. UV-Vis (λ_{max}, nm): 270 (π–π* of aromatic rings).

N1,N3-bis(1-hydrazinyl-1-oxopropan-2-yl)isophthalamide Mn(II) chloride $[Mn(H_2L)(H_2O)_2].Cl_2$; Yield 86%; m.p. 288 °C; Off-white solid. Anal. Calc. for $C_{14}H_{24}Cl_2MnN_6O_6$ (%): C, 33.75; H, 4.86; N, 16.86; M, 11.03. Found (%): C, 33.75; H, 4.81; N, 16.87; M, 10.98. FT-IR (KBr, ν, cm^{-1}) 3080(NH stretching), 2936 (CH, aromatic), 2094 (CH aliphatic) and 1780 (CONH), 1560 (NH2), 540 (M─O), 440 (M─N). μ_{eff} (BM) 5.20; Λ_m (Ω^{-1} mol^{-1} cm^2) 115. UV-Vis (λ_{max}, nm): 270 (π–π* of aromatic rings).

2.6. Spectrophotometric studies

The absorption spectra were recorded for 1×10^{-4} M solutions of the ligand and metal complexes. The spectra were scanned within the wavelength range from 200 to 700 nm.

2.7. Molecular docking

AutoDock 4.2 and docking computations applying Gasteiger partial charges added to ligand (designed drug) atoms were used as previously described [21, 22].

2.8. Biological Activity

The diffusion agar method was used to test the biological activity of the ligand and complexes and the details of the method were previously described. The antibacterial activities were calculated as a mean of three replicates and the MIC_{50} was determined [23-27].

2.9. Computational methodology:

The optimized structural geometry of the ligand was determined using the DFT/B3LYP method with different base sets using Gaussian09 software [28] and the significant bond lengths, oscillator strengths, excitation energies and effective charges for coordinating groups in optimized structures were deduced.

2.10. Molecular Docking

AutoDock 4.2 and docking computations applying Gasteiger partial charges added to ligand (designed drug) atoms were used as described previously [29-32].

3. Results and discussion

The synthesized ligand (H_2L) was characterized using elemental analysis (C, H, N), infrared spectral studies (IR), ^1H and ^{13}C NMR, mass spectra and thermal analysis (TG and DTG) as previously described. The optimized geometrical structure and numbering of the ligand using molecular modeling with the Gaussian09 program was given in Figure (1) and Figure (2) [33, 34] and the data obtained were given in the previous study.

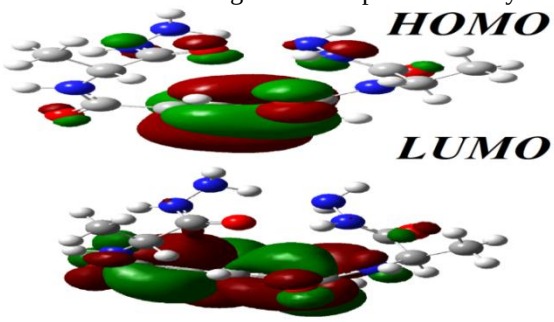

Figure (1) the optimized geometrical structure of the ligand using molecular modeling

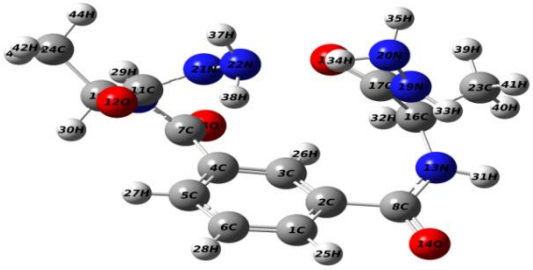

Figure (2) Numbering of the ligand using molecular modeling

3.1. Characterization of metal complexes

The physical, analytical and spectroscopic data of the complexes were summarized in the experimental part(Table (1)). They are air stable and soluble in DMF and DMSO solvents but insoluble in MeOH, EtOH, acetone, CCl_4 and benzene. There is satisfactory agreement between the calculated and found percentages elemental analyses data which confirmed the formation of complexes in 1 M : 1 L ratio [35-40].

Complex	Color (% yield)	M.P (°C)	% Calcd. (Found)				μeff (B.M)	Λm $\Omega^{-1}mol^{-1}cm^2$
			C	H	N	M		
H_2L	White (82)	110	49.99 (49.92)	5.99 (5.93)	24.99 (24.94)	-		
$[Cu(H_2L)(H_2O)_2]Cl_2$ C14H24Cl2CuN6O6	DarkBlue (88)	279	33.18 (33.14)	4.77 (4.70)	16.58 (16.52)	12.54 (12.49)	1.84	115
$[Cd(H_2L)(H_2O)_2]Cl_2$ C14H24CdCl2N6O6	White green (88)	281	30.26 (30.21)	4.35 (4.29)	15.12 (15.07)	20.23 (20.19)	Diam	75
$[Mn(H_2L)(H_2O)_2]Cl_2$ C14H24Cl2MnN6O6	Off-white (86)	288	33.75 (33.02)	4.86 (4.81)	16.87 (16.82)	11.03 (10.98)	5.20	115

Table (1). Elemental and physical data of ligand metal complexes

3.2. IR spectral studies

The IR spectra of the ligand and metal complexes were carried out in the range of 4000-400 cm^{-1}, and the most effective bands are given in the experimental part. The sharp stretching vibration bands observed at 3070-3080 cm^{-1} (3050 cm^{-1} in the free ligand) indicating that the ligand coordinates to metal ions via amine moiety. The complexes exhibited bands in the range of 1767 -1780 cm^{-1} in comparison with the free ligand at 1740 cm^{-1} which attributed to the amide (C=ONH) group. This shift in band position confirmed that the complexation reaction occurred through formation of coordinate bond with nitrogen oxygen atoms of the ligand [41]. The medium and week bands found in the spectra of the complexes in the range of 532-540 cm^{-1} and 430-440 cm^{-1} can assigned to ν(M-O) and ν(M-N) stretching vibrations, respectively [42-46]. According to the above data, it can conclude that the ligand behaved as neutral tetradentate ligand and coordinated to the metal ions via the tow amide nitrogen atoms and the two carbonyl oxygen atoms to the metal ions.

3.3. ^{1}H-NMR spectra:

The ^{1}H-NMR spectrum of the ligand was compared with that of Cd(II) complexe and the data obtained revealed that the signals still appeared at the same position as the ligand but enhancement decrease which support the coordination of ligand to metal ions with protonated amide group. [47]

3.4. Molar conductivity measurements

In order to detect if the counter ions either outside or inside the coordination sphere, the conductivity measurements must be measured where it can indicate the degree of ionization of the prepared complexes. The molar conductivity of 1×10^{-3} M solutions of the prepared metal complexes in DMF solvent was measured and was found to be were 115, 75 and 115 Ω^{-1} cm^2 mol^{-1} for Cu (II), Cd(II) and Mn(II) complexes, respectively. These data supported the electrolytic nature of the complexes.

3.5. Electronic spectra and magnetic moment measurements:

It is possible to draw up the electronic transitions and detect the geometry with the help of magnetic moments of most metal ions [48]. The experimental magnetic moment value of 1.84 B.M. for Cu(II) complex represented the presence of one unpaired electron per Cu(II) ion for d^9 system suggesting spin-free distorted octahedral geometry. The diffused reflectance spectrum of this complex indicated the d–d transition bands at 13,970, 20,140 and 25,132 cm^{-1}. The bands appeared correspond to $^2B_{1g}\rightarrow{}^2A_{1g}$ (dx^2-$y^2\rightarrow dz^2$), $^2B_{1g}\rightarrow{}^2B_{2g}$ (dx^2-$y^2\rightarrow$dxy) and $^2B_{1g}\rightarrow{}^2E_g$ (dx^2–$y^2\rightarrow$dxz, dyz) transitions, respectively. These data suggested an octahedral geometry of the Cu(II) complex The diffused reflectance spectrum of the Mn(II) complex pointed out three bands at 13,256, 18,420 and 21,253 cm^{-1} which are assigned to $^4A_{1g}\rightarrow{}^6A_{1g}$, $^4T_{2g}$ (G)$\rightarrow{}^6A_{1g}$ and $^4T_{1g}$ (D)$\rightarrow{}^6A_{1g}$ transitions, respectively. It has μ_{eff} value of 5.17 B.M. which confirmed octahedral geometry of the Mn(II) complex [49]. Cd(II) complex is diamagnetic and according to their empirical formula, they have octahedral geometry.

3.6. Mass spectral studies:

The mass of spectra of the for $[Cu(H_2L)(H_2O)_2].Cl_2$, $[Cd(H_2L)(H_2O)_2].Cl_2$ and $[Mn(H_2L)(H_2O)_2].Cl_2$ complexes showed molecular ion peaks at m/z 505.04, 556.02 and 497.05 amu, respectively. Their spectra of the complexes showed also molecular ion (m/z) peaks at 336.15 amu corresponding to the ligands which further support complex formation (Figure 2).

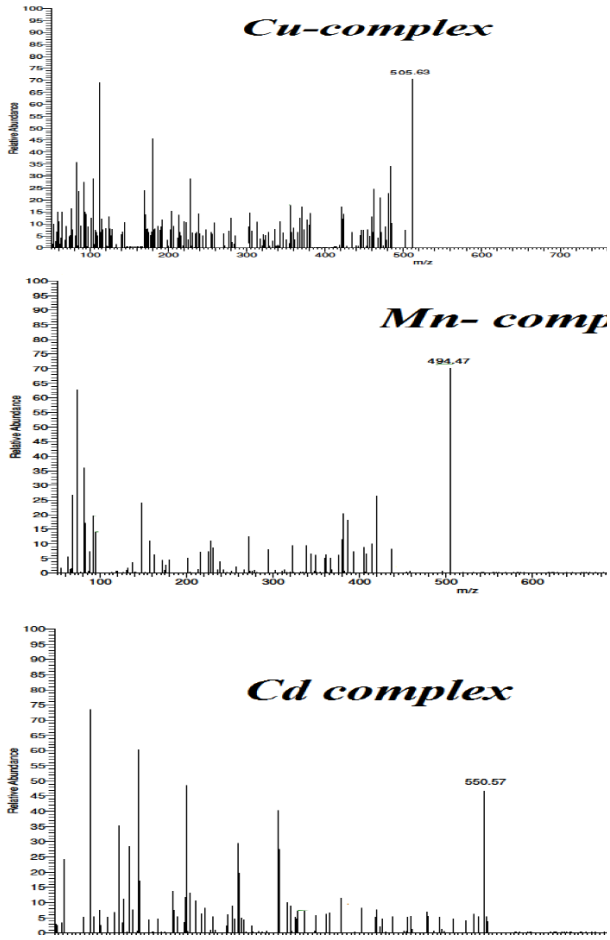

Figure (3). Mass of metal complexes

3.7. UV-Visible spectra of the azo dye ligand and its metal complexes

The UV-visible spectrum of the ligand showed sharp peak at 276 nm that corresponding to π-π* transitions within the phenyl and azomethine groups [50-55]. This peak was found in the complexes at 270 nm indicated the participation of azomethine group in coordination.

3.8. Thermal analysis studies (TG and DTG):

The TG data for the ligand (H_2L) showed four steps of decomposition. The first step within the temperature range of 40-220 °C with temperature maximum 150°C, was correlated with evaluation ofC_7H_8molecules with mass loss of 27.38% (calcd. 28.31%).The second decomposition step within the temperature range of220–600°C correspond to decomposition of sequence parts of ligand (NO and C_4 H_4molecules) with mass loss of43.85% (calcd43.45%). The last step of decomposition within the temperature range of 600-1000°C corresponds to the molecules of the ligand with mass loss of 26.82% (calcd30.05%).The total weight loss amounted to 89.98%% (calcd. 100.88%).

The TG thermogram of $[Cu(H_2L)(H_2O)_2]Cl_2$ complex showed four decomposition steps. The first decomposition step accompanied by loss of C_4H_8 and $2H_2O$.molecules in the temperature range of 45-200 °C with an estimated weight loss of 17.31% (calcd. 18.21%). The second decomposition step accompanied by loss of 2HCl, N_2O and CH_2 molecules in the temperature range of 200-450 °C with an estimated weight loss of 25.52% (calcd. 25.74%). The third and fourth steps of decomposition showed loss of $C_7H_6N_4$ and $C_2H_2O_2$ molecules at 450-650 °C and 650-1000 °C with an estimated weight loss of 30.46% (calcd. 28.91%) and 11.07% (calcd. 11.68). Thereafter, the percentage of the residue corresponds to cadmium oxide and the total approximate weight loss was found to be 84.36% (calcd. 84.54%).

The TG thermogram of $[Cd(H_2L)(H_2O)_2]Cl_2$ complex showed four decomposition steps. The first decomposition step accompanied by loss of $2H_2O$ and 2HCL molecules in the temperature range of 40-210 °C with an estimated weight loss of 18.88% (calcd. 19.78%). The second decomposition step was accompanied by loss of **$2H_2O$ and 2HCL**. molecules in the temperature range of 210-610 °C with an estimated weight loss of 22.61% (calcd. 23.74%). The third step of decomposition showed loss of **$C_7H_{10}N_2O$** molecule at 610-800 °C with an estimated weight loss of 24.34% (calcd. 24.82%). The fourth step of decomposition showed loss of **C_4H_2** molecule at 800-1000 °C with an estimated weight loss of 11.15% (calcd. 8.99%). Thereafter, the percentage of the residue corresponds to zinc oxide contaminated with carbon and the total approximate weight loss was found to be 76.98% (calcd. 77.33%).

The TG thermogram of $[Mn(H_2L)(H_2O)_2]Cl_2$ complex showed three decomposition steps. The first decomposition step accompanied by loss of 2HCL and $2H_2O$ molecules in the temperature range of 50-280 °C with an estimated weight loss of 21.88% (calcd. 22.33%). The second decomposition step accompanied by loss of N_2O and C_4H_8 molecules in the temperature range of 280-600 °C with an estimated weight loss of 35.46% (calcd. 37.82%). The last step of decomposition showed loss of $C_{10}H_{10}$ molecule at 600-1000 °C with an estimated weight loss of 28.38% (calcd. 26.15%). Thereafter, the percentage of the residue corresponds to manganese oxide contaminated with carbon and the total approximate weight loss was found to be 85.72% (calcd. 86.30%).

Compound	TG range (°C)	DTG_{max} (°C)	n *	Mass Loss Total mass Loss Calcd (Estim) %	Assignment	residue
H_2L	40–220 220–600 600-1000	150 380 750	1 1 1	27.38 (28.31) 43.45 (43.85) 100.88(89.98) 30.05 (26.82)	- Loss of C_7H_8 - Loss of NO and C_4H_4 -Loss of $C_4H_6N_4O_2$ -Loss of $C_3H_6N_2O_2$	
$[Cu(H_2L)(H_2O)_2]Cl_2$	45-200 200-450 450-650 650-1000	150 300 520 750	1 1 1 1	18.21 (17.31) 25.74 (25.52) 28.91 (30.46) 84.54 (84.36) 11.68 (11.07)	- Loss of C_4H_8 and $2H_2O$. - Loss of 2HCl, N_2O and CH_2 - Loss of $C_7H_6N_4$. - Loss of $C_2H_2O_2$	CuO
$[Cd(H_2L)(H_2O)_2]Cl_2$	40-210 210-610 610-800 800-1000	150 4000 650 880	1 1 1 1	19.78 (18.88) 23.74 (22.61) 24.82 (24.34) 77.33 (76.98) 8.99 (11.15)	- Loss of $2H_2O$ and 2HCL. - Loss of N_2O and C_3H_6. - Loss of $C_7H_{10}N_2O$. - Loss of C_4H_2.	CdO
$[Mn(H_2L)(H_2O)_2]Cl_2$	50-280 280-600 600-1000	180 350 800	1 1 1	22.33 (21.88) 37.82 (35.46) 86.30 (85.72) 26.15 (28.38)	- Loss of 2HCL and $2H_2O$. - Loss of N_2O and C_4H_8 - Loss of $C_{10}H_{10}$.	MnO

TABLE 2. Thermoanalytical results (TG, DTG and DTA) for ligand and metal complexes

3.9. Structura1 interpretation

According to the analytical and spectroscopic data previously described, the proposed structures of metal complexes were given in Figure 4.

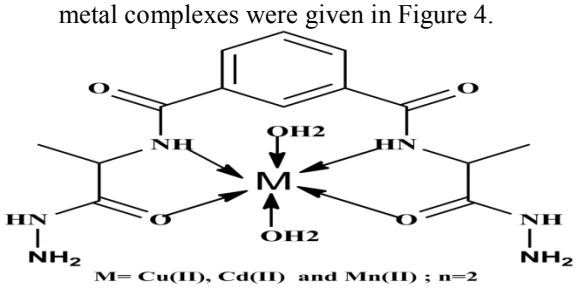

Figure 4 Structure of metal complexes of ligand.

3.10. Molecular Docking

Auto Dock is considered as one of the modern methods used to illustrate and demonstrate the benefits of biological features of Schiff bases and metal complexes and shed light on experimental data. Docking was applied for ligand (guest) with different kinds of organisms (various protein receptors) as host such as: Bacillus subtilis (5ZW4-A), Escherichia coli (3HUM-A), Pseudomonas aeruginosa (4WEL-A) and Staphylococcus aureus (5M18-A). Also, the energies for the docking procedure can be calculated. The strong interaction with all receptors with comparable results can be determined from HB plots (Figures 5–8) according to computation. Inter-hydrogen bonding was clearly visible for all proteins. The mode of interaction inside the docking molecules can be visualized by two-dimensional plots (Figures 5–8).

It appeared that the interaction occurred between the amino acids of proteins and the ligand via hydrogen bonds as follows: Bacillus subtilis (5ZW4-A), Escherichia coli (3HUM-A), Pseudomonas aeruginosa (4WEL-A) and Staphylococcus aureus (5M18-A): amino acid of protein reacted with ligand by H-bond of Bacillus subtilis (5ZW4-A): 5zw4-pdb-H//A/ARG`90/2HH2– with hydrogen bond length 2.3 $A^o$, 5zw4-pdb-H//A/GLU`85/OE1– with hydrogen bond length 3.3 A^o, 5zw4-pdb-H//A/GLU`85/OE1– with hydrogen bond length 2.1 $A^o$, 5zw4-pdb-H//A/GLU`85/OE2– with hydrogen bond length 2.4 A^o, 5zw4-pdb-H//A/ARG`86/HE– with hydrogen bond length 2.3 $A^o$, 5zw4-pdb-H//A/ARG`86/HE– with hydrogen bond length 2.6 A^o, 5zw4-pdb-H//A/ASP`133/OD1– with hydrogen bond length 2.8 $A^o$, 5zw4-pdb-H//A/ASP`133/OD1– with hydrogen bond length 2.4 A^o, 5zw4-pdb-H//A/ASP`159/OD2– with hydrogen bond length 2.5 $A^o$, 5zw4-pdb-H//A/ASP`208/OD2– with hydrogen bond length 2.9 A^o, 5zw4-pdb-

H//A/ILE`37/O– with hydrogen bond length 3.5 A°, with binding energy = −7.4 kcal mol−1 (Figures 5–8).

For E. coli (3HUM-A): the amino acids of protein reacted with ligand by H-bond as follow: 1-3hum-A-h//A/GLU`114/O– with hydrogen bond length 2.9 A°, 3hum-A-h//A/GLU`114/O– with hydrogen bond length 3.4 A°, 3hum-A-h//A/SER`116/HN– with hydrogen bond length 2.4 A°, 3hum-A-h//A/SER`116/HN – with hydrogen bond length 2.7A°, 3hum-A-h//A/SER`75/HG – with hydrogen bond length 2.0 A°, 3hum-A-h//A/SER`139/HG – with hydrogen bond length 2.2 A°, 3hum-A-h//A/GLU`297/OE2 – with hydrogen bond length 2.4 A°, 3hum-A-h//A/GLU`297/OE2 – with hydrogen bond length 3.1 A°, 3hum-A-h//A/GLU`297/OE1 – with hydrogen bond length 3.2 A°, 3hum-A-h//A/TYR`268/OH – with hydrogen bond length 2.2 A°, 3hum-A-h//A/TYR`268/OH – with hydrogen bond length 2.2 A°, with binding energy = − 7.6 kcal mol− 1. (Figures 5–8)

For P. aeruginosa (4wel): amino acid of protein reacts with ligand by H-bond: 4wel-h//A/PRO`516/O– with hydrogen bond length 2.5 A°, 4wel-h//A/ASP`515/OD1– with hydrogen bond length 2.5 A°, 4wel-h//A/LYS`255/HZ2– with hydrogen bond length 2.4 A°, 4wel-h//A/ASN`427/1HD2– with hydrogen bond length 2.5 A°, 4wel-h//A/ALA`426/O– Length 2.6 A°, 4wel-h//A/ASP`428/OD1– with hydrogen bond length 3.4 A°, 4wel-h//A/GLN`458/1HE2– with hydrogen bond length 2.1 A°, 4wel-h//A/THR`514/O– with hydrogen bond length 2.6 A°, 4wel-h//A/ALA`513/O– with hydrogen bond length 2.4 A°, with binding energy = 5.6 kcal mol−1. (Figures 5–8)

For S. aureus (5M18-A): amino acid of protein reacted with ligand by H- bond: 5M18-A-h//A/THR`238/OG1– with hydrogen bond length 2.5 A°, 5M18-A-h//A/GLU`239/O– with hydrogen bond length 2.4 A°, 5M18-A-h//A/GLU`239/O– with hydrogen bond length 2.6 4°, 5M18-A-h//A/GLU`239/O– with hydrogen bond length 2.4 A°, 5M18-A-h//A/THR`165/HG1– with hydrogen bond length 2.1 A°, 5M18-A-h//A/ARG`151/HN– with hydrogen bond length 2.3 A°, 5M18-A-h//A/SER`149/O– with hydrogen bond length 2.1 A°, with binding energy = − 7.8 kcal mol− 1. (Figures 5–8)

3.13. Antimicrobial activity

Ligands that have donor atoms like oxygen and nitrogen are an important class of compounds as they have wide range of applications in the medicinal field. They display biological activities as antibacterial [56, 57] and antitumor activities. Microbes are exposed to or confronted with a variety of different metal ions in the surrounding environment, which in turn interact with them, and are often useful to humans and sometimes others are more dangerous and damaging. The benefit and damage depend on their nature, whether chemical or physical, and also on the state of oxidation of the metal ion. It is very necessary to study the presence of these ions and how to find them, and it is observed that they are often found as cations (or cationic compounds) or oxy anions, such as salts or oxides in crystalline form or insoluble deposits in an insoluble form.

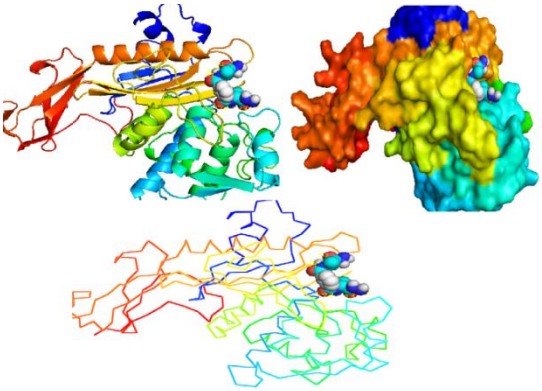

Figure 5 Three-dimensional plot of interaction of ligand with (3HUM-A)E. coli receptor.

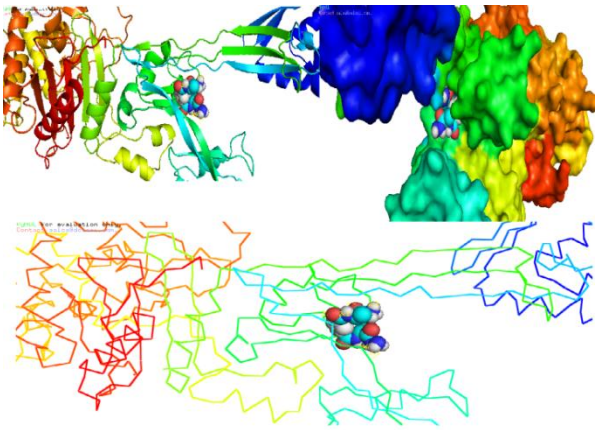

Figure 6 Three-dimensional plot of interaction of ligand with (5M18-A). aureus receptor

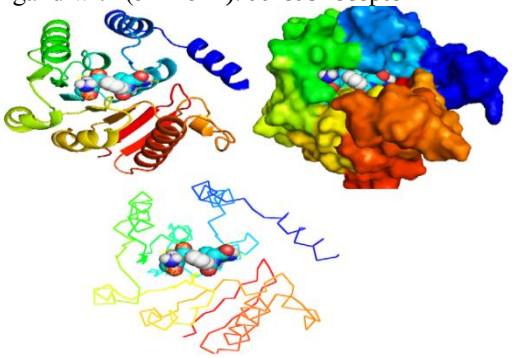

Figure 7 Three-dimensional plot of interaction of ligand with (5ZW4-A) B. subtilis receptor

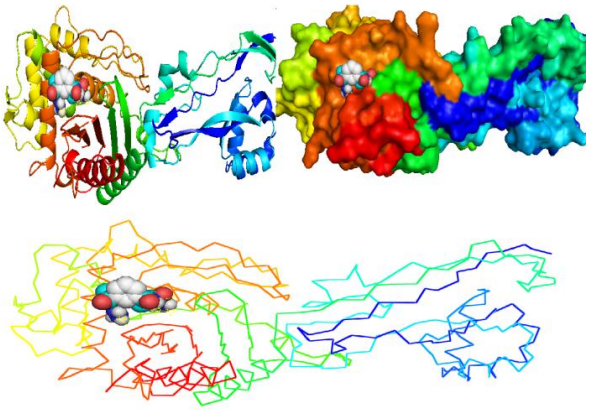

Figure 8 Three-dimensional plot of interaction of ligand with (4we)l P. aeruginosa receptor

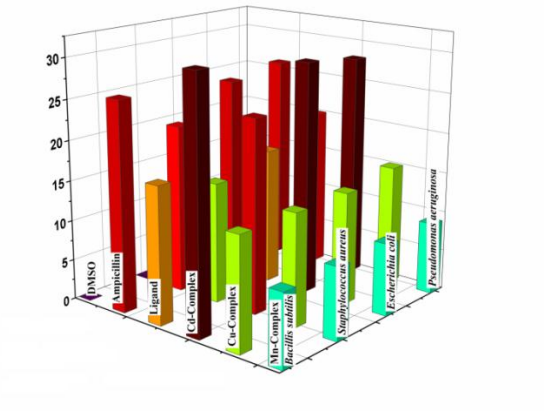

FIGURE 9 Biological activities of ligand and its metal complexes.

From the study of these microbes, it is found that they have a great ability to overlap and bind the metal ions in the external environment on the surface of cells and transferred to the cell for different functions within the cells. All microbes, whether eukaryotic or eukaryotic, use metals for structural and/or catalytic functions. Antimicrobial activity was determined for the ligand and its complexes using the diffusion agar method [58-60].

Ampicillin was considered as a reference biochemical antibiotic for antibacterial activities. In examining the antibacterial activity of these complexes, more than one organism is used to increase the chance of detecting antibiotic activities in the test materials. Gram-positive (*S. aureus* ATTC12600 and *B. subtilis* ATTC 6051) and Gram-negative (*P. aeruginosa* ATTC 13315 and *E. coli* ATTC 11775) bacteria were used as test organisms. The antibacterial behavior was estimated by evaluating the inhibition zone diameter (mm) and minimum inhibitory concentration (MIC_{50}) (Figure 9). It was observed that the ligand has less activity towards Gram-positive and toward Gram-negative bacteria as can see from Figure (9). The activity of Cd(II) complex is higher than ligand, Cu(II) complex than Mn(II) towards *B. subtilis*, *S. aureus*, *E. coli* and *P. aeruginosa* organisms with inhibition zone values of 31, 24, 29 and 28 mm/mg, respectively, for Cd(II) complex and inhibition zone values of 17, 15, 17 and 20 mm/mg, respectively, for ligand. Whereas Cu(II) complex has inhibition zone values of 14, 14, 14 and 15 mm/mg, respectively towards *B. subtilis*, *S. aureus*, *E. coli* and *P. aeruginosa* organisms. Whereas Mn(II) complex has inhibition zone values of 9, 9, 9 and 9 mm/mg, respectively towards *B. subtilis*, *S. aureus*, *E. coli* and *P. aeruginosa* organisms.

4. Conclusion

In order to classify the ligand under investigation and its transition metal complexes, various physicochemical, spectroscopic and thermal methods of analysis were used. In addition, the [Cd $(H_2L)(H2O)_2]Cl_2$ complex was classified as the most active antibacterial/antifungal compound among them when researching their antimicrobial activities. Docking studies of ligands were investigated, revealing that ligand activity varies depending on the kind of protein, with the lowest binding energy that can interact with multiple receptors in the proteins analyzed.

References

[1] J. Hajduch, B. Fabre, B. Klopp, R. Pohl, M. Buděšínský, V. Šolínová, V. Kašička, C. Köprülüoglu, S.M. Eyrilmez, M. Lepšík, Multipodal insulin mimetics built on adamantane or proline scaffolds, Bioorganic chemistry 107 (2021) 104548.

[2] G. Viault, S. Dautrey, N. Maindron, J. Hardouin, P.-Y. Renard, A. Romieu, The first "ready-to-use" benzene-based heterotrifunctional cross-linker for multiple bioconjugation, Organic & biomolecular chemistry 11(16) (2013) 2693-2705.

[3] E. Nixon, J.W. Simpkins, Neuroprotective effects of nonfeminizing estrogens in retinal photoreceptor neurons, Investigative ophthalmology & visual science 53(8) (2012) 4739-4747.

[4] H. Abdelsalaam, E.M. Zayed, M. Zayed, M. Nouman, Synthesis, structural characterization, thermal behaviour and antimicrobial activity of copper, cadmium and zinc chelates of traizole-thiole ligand in comparison with theoretical molecular orbital calculations, Egyptian Journal of Chemistry 62(Special Issue (Part 1) Innovation in Chemistry) (2019) 145-163.

[5] E.M. Zayed, M.A. Zayed, A.M. Hindy, G.G. Mohamed, Coordination behaviour and biological

activity studies involving theoretical docking of bis-Schiff base ligand and some of its transition metal complexes, Applied Organometallic Chemistry 32(12) (2018) e4603.
[6] G. Gamov, A. Kiselev, V. Aleksandriisky, V. Sharnin, Influence of regioisomerism on stability, formation kinetics and ascorbate oxidation preventive properties of Schiff bases derived from pyridinecarboxylic acids hydrazides and pyridoxal 5′-phosphate, Journal of Molecular Liquids 242 (2017) 1148-1155.
[7] P.A. Clemons, N.E. Bodycombe, H.A. Carrinski, J.A. Wilson, A.F. Shamji, B.K. Wagner, A.N. Koehler, S.L. Schreiber, Small molecules of different origins have distinct distributions of structural complexity that correlate with protein-binding profiles, Proceedings of the National Academy of Sciences 107(44) (2010) 18787-18792.
[8] Z. Vargová, R. Gyepes, L. Arabuli, K. Györyová, P. Hermann, I. Lukeš, Synthesis, crystal structures and spectroscopic properties of three Zn–cyclen–aminoacid complexes with new macrocyclic configurations, Inorganica Chimica Acta 362(10) (2009) 3860-3866.
[9] D.K. Mahapatra, S.K. Bharti, V. Asati, Chalcone derivatives: anti-inflammatory potential and molecular targets perspectives, Current topics in medicinal chemistry 17(28) (2017) 3146-3169.
[10] E.M. Zayed, A.M. Hindy, G.G. Mohamed, coordination behaviour, molecular docking, density functional theory calculations and biological activity studies of some transition metal complexes of bis-Schiff base ligand, Applied Organometallic Chemistry 33(1) (2019) e4525.
[11] H.M.A. Abosadiya, B.M. Yamin, SYNTHESIS AND MOLECULAR STRUCTURE OF THE COMPLEXES OF TRIMETHYL-AND TRIBUTYLTIN CHLORIDE WITH 3-(3-BENZOYL THIOUREIDO) PROPIONIC ACID, Jurnal Sains MIPA Universitas Lampung 5(2) (2012).
[12] J. van Schijndel, L.A. Canalle, D. Molendijk, J. Meuldijk, Exploration of the role of double schiff bases as catalytic intermediates in the knoevenagel reaction of furanic aldehydes: mechanistic considerations, Synlett 29(15) (2018) 1983-1988.
[13] H.S. Alsaeedi, N.A. Aljaber, I. Ara, Synthesis and investigation of antimicrobial activity of some nifuroxazide analogues, Asian Journal of Chemistry 27(10) (2015) 3639-3646.
[14] J. van Schijndel, D. Molendijk, K. van Beurden, L.A. Canalle, T. Noël, J. Meuldijk, Preparation of bio-based styrene alternatives and their free radical polymerization, European Polymer Journal 125 (2020) 109534.
[15] A.M. Farag, H.H. Sokker, E.M. Zayed, F.A.N. Eldien, N.M. Abd Alrahman, Removal of hazardous pollutants using bifunctional hydrogel obtained from modified starch by grafting copolymerization, International journal of biological macromolecules 120 (2018) 2188-2199.
[16] S.L. Gaonkar, U. Vignesh, Synthesis and pharmacological properties of chalcones: a review, Research on chemical intermediates 43(11) (2017) 6043-6077.
[17] Ehab M. Zayed, Gehad G. Mohamed, Synthesis, spectroscopic, DFT and docking studies, Molecular structure of new Schiff base metal complexes, Egyptian Journal of Chemistry 65(1) (2022) 633.
[18] A. Pawlak, M. Henklewska, B. Hernández Suárez, M. Łużny, E. Kozłowska, B. Obmińska-Mrukowicz, T. Janeczko, Chalcone Methoxy Derivatives Exhibit Antiproliferative and Proapoptotic Activity on Canine Lymphoma and Leukemia Cells, Molecules 25(19) (2020) 4362.
[19] B. Zhou, C. Xing, Diverse molecular targets for chalcones with varied bioactivities, Medicinal chemistry 5(8) (2015) 388.
[20] G. O Moustafa, Therapeutic potentials of cyclic peptides as promising anticancer drugs, Egyptian Journal of Chemistry (2021).
[21] M.I. Alkhalaf, Attenuating effect of Indole-3-Carbinol on gold nanoparticle induced hepatotoxicity in rats, Arabian Journal of Chemistry 13(11) (2020) 8060-8068.
[22] E.M. Zayed, M.A. Zayed, A.M. Fahim, F.A. El-Samahy, Synthesis of novel macrocyclic Schiff's-base and its complexes having N2O2 group of donor atoms. Characterization and anticancer screening are studied, Applied Organometallic Chemistry 31(9) (2017) e3694.
[23] A.R. Chacko, J. Jeyakanthan, G. Ueno, K. Sekar, C.D. Rao, E.J. Dodson, K. Suguna, R.J. Read, A new pentameric structure of rotavirus NSP4 revealed by molecular replacement, Acta Crystallographica Section D: Biological Crystallography 68(1) (2012) 57-61.
[24] E.M. Zayed, F.A. El-Samahy, G.G. Mohamed, Structural, spectroscopic, molecular docking, thermal and DFT studies on metal complexes of bidentate orthoquinone ligand, Applied Organometallic Chemistry 33(9) (2019) e5065.
[25] N. Nikooei, M.G. Dekamin, E. Valiey, Benzene-1, 3, 5-tricarboxylic acid-functionalized MCM-41 as a novel and recoverable hybrid catalyst for expeditious and efficient synthesis of 2, 3-dihydroquinazolin-4 (1 H)-ones via one-pot three-component reaction, Research on Chemical Intermediates 46 (2020) 3891-3909.
[26] K.M. Khan, M.T. Muhammad, I. Khan, S. Perveen, W. Voelter, Rapid cesium fluoride-catalyzed Knoevenagel condensation for the synthesis of highly functionalized 4, 4′-(arylmethylene) bis (1 H-pyrazol-5-ol)

derivatives, Monatshefte für Chemie-Chemical Monthly 146(9) (2015) 1587-1590.
[27] E.M. Aleassa, M. Hassan, K. Hayes, S.A. Brethauer, P.R. Schauer, A. Aminian, Effect of revisional bariatric surgery on type 2 diabetes mellitus, Surgical endoscopy 33(8) (2019) 2642-2648.
[28] E.M. Zayed, M. Zayed, H.A. Abd El Salam, M.A. Noamaan, Novel Triazole Thiole ligand and some of its metal chelates: Synthesis, structure charactertization, thermal behavior in comparison withcomputational caculations andbiological activities, Computational biology and chemistry 78 (2019) 260-272.
[29] E.M. Zayed, M. Zayed, Synthesis of novel Schiff's bases of highly potential biological activities and their structure investigation, Spectrochimica Acta Part A: Molecular and Biomolecular Spectroscopy 143 (2015) 81-90.
[30] I. Borges, J. Danielli, V. Silva, L. Sallum, J. Queiroz, L. Dias, I. Iermak, G. Aquino, A. Camargo, C. Valverde, Synthesis and structural studies on (E)-3-(2, 6-difluorophenyl)-1-(4-fluorophenyl) prop-2-en-1-one: a promising nonlinear optical material, RSC Advances 10(38) (2020) 22542-22555.
[31] S. Bhattacharya, A.P. Sherje, Development of resveratrol and green tea sunscreen formulation for combined photoprotective and antioxidant properties, Journal of Drug Delivery Science and Technology 60 (2020) 102000.
[32] E.K. Kazakova, J.E. Morozova, D.A. Mironova, A.I. Konovalov, Sorption of azo dyes from aqueous solutions by tetradodecyloxybenzylcalix [4] resorcinarene derivatives, Journal of Inclusion Phenomena and Macrocyclic Chemistry 74(1-4) (2012) 467-472.
[33] E.M. Zayed, E.H. Ismail, G.G. Mohamed, M.M. Khalil, A.B. Kamel, Synthesis, spectroscopic and structural characterization, and antimicrobial studies of metal complexes of a new hexadentate Schiff base ligand. Spectrophotometric determination of Fe (III) in water samples using a recovery test, Monatshefte für Chemie-Chemical Monthly 145(5) (2014) 755-765.
[34] E.M. Zayed, G.G. Mohamed, A.M. Hindy, Transition metal complexes of novel Schiff base, Journal of Thermal Analysis and Calorimetry 120(1) (2015) 893-903.
[35] Y. Kim, K. Hyun, D. Ahn, R. Kim, M.H. Park, Y. Kim, Efficient aluminum catalysts for the chemical conversion of CO2 into cyclic carbonates at room temperature and atmospheric CO2 pressure, ChemSusChem 12(18) (2019) 4211-4220.
[36] J. Sim, M. Viji, J. Rhee, H. Jo, S.J. Cho, Y. Park, S.Y. Seo, K.Y. Jung, H. Lee, J.K. Jung, γ-Functionalization of α, β-Unsaturated Nitriles under Mild Conditions: Versatile Synthesis of 4-Aryl-2-Bromopyridines, Advanced Synthesis & Catalysis 361(23) (2019) 5458-5465.
[37] S. Ding, Z. Ni, M. Hu, G. Qiu, J. Li, J. Ye, X. Zhang, F. Liu, H. Dong, W. Hu, An Asymmetric Furan/Thieno [3, 2-b] Thiophene Diketopyrrolopyrrole Building Block for Annealing-Free Green-Solvent Processable Organic Thin-Film Transistors, Macromolecular rapid communications 39(15) (2018) 1800225.
[38] E.M. Zayed, G.G. Mohamed, W.M. Hassan, A.K. Elkholy, H. Moustafa, Spectroscopic, thermal, biological activity, molecular docking and density functional theoretical investigation of novel bis Schiff base complexes, Applied Organometallic Chemistry 32(7) (2018) e4375.
[39] E.M. Zayed, M. Zayed, A.M. Hindy, Thermal and spectroscopic investigation of novel Schiff base, its metal complexes, and their biological activities, Journal of Thermal Analysis and Calorimetry 116(1) (2014) 391-400.
[40] M.A. Gouda, G.E. Abd El-Ggani, M.A. Berghot, A.E.G.M. Khalil, Synthesis and Antioxidant Activity of Some Novel Nicotinonitrile Derivatives Bearing a Furan Moiety, Journal of Heterocyclic Chemistry 56(7) (2019) 2036-2045.
[41] W. Al Zoubi, A.A.S. Al-Hamdani, I. Putu Widiantara, R.G. Hamoodah, Y.G. Ko, Theoretical studies and antibacterial activity for Schiff base complexes, Journal of Physical Organic Chemistry 30(12) (2017) e3707.
[42] F.M. Almutairi, A.G. Ali, A.O. Abdelhamid, A.I. Alalawy, M.K. Bishr, M.S. Mohamed, The Identification of a Novel Unsymmetrical Azine as an Apoptosis Inducer in Colorectal Cancer, Anti-Cancer Agents in Medicinal Chemistry (Formerly Current Medicinal Chemistry-Anti-Cancer Agents) 21(3) (2021) 406-413.
[43] E.M. Zayed, A.M. Hindy, G.G. Mohamed, Molecular structure, molecular docking, thermal, spectroscopic and biological activity studies of bis-Schiff base ligand and its metal complexes, Applied Organometallic Chemistry 32(1) (2018) e3952.
[44] M. Khajehzadeh, N. Sadeghi, Molecular structure, the effect of solvent on UV–vis and NMR, FT–IR and FT–Raman spectra, NBO, frontier molecular orbital analysis of Mitomycin anticancer drug, Journal of Molecular Liquids 256 (2018) 238-246.
[45] E.M. Zayed, M. Zayed, M. El-Desawy, Preparation and structure investigation of novel Schiff bases using spectroscopic, thermal analyses and molecular orbital calculations and studying their biological activities, Spectrochimica Acta Part A: Molecular and Biomolecular Spectroscopy 134 (2015) 155-164.
[46] S. Chen, Y. Xia, B. Zhang, H. Chen, G. Chen, S. Tang, Disassembly of lignocellulose into cellulose, hemicellulose, and lignin for

preparation of porous carbon materials with enhanced performances, Journal of Hazardous Materials 408 (2021) 124956.
[47] W.M. Hassan, E.M. Zayed, A.K. Elkholy, H. Moustafa, G.G. Mohamed, Spectroscopic and density functional theory investigation of novel Schiff base complexes, Spectrochimica Acta Part A: Molecular and Biomolecular Spectroscopy 103 (2013) 378-387.
[48] A. Grandāne, A. Nocentini, I. Domračeva, R. Žalubovskis, C.T. Supuran, Development of oxathiino [6, 5-b] pyridine 2, 2-dioxide derivatives as selective inhibitors of tumor-related carbonic anhydrases IX and XII, European Journal of Medicinal Chemistry 200 (2020) 112300.
[49] G. Maiti, U. Kayal, R. Karmakar, R.N. Bhattacharya, Terminal alkynes as keto-methyl equivalent toward one pot synthesis of 1, 5-benzodiazepine derivatives under catalysis of Hg (OTf) 2, Tetrahedron Letters 53(12) (2012) 1460-1463.
[50] I. Vencato, P.H. Ferri, S.C. Santos, M. Pereira, C. Lariucci, L.I. Homar, H.B. Napolitano, 1-(4-Methoxyphenyl)-2-(6-methyl-2-nitro-3-pyridyloxy) propan-1-one, Acta Crystallographica Section E: Structure Reports Online 61(2) (2005) o247-o249.
[51] V.S. Duarte, G.D. D'Oliveira, J.M. Custodio, S.S. Oliveira, C.N. Perez, H.B. Napolitano, Experimental and molecular modeling study of a novel arylsulfonamide chalcone, Journal of molecular modeling 25(7) (2019) 1-14.
[52] M. Kumari, S. Jain, Development of tannin containing nutraceutical additive from Babul (Acacia nilotica) and its acceptability in food products for management of Diabetes, Medicinal Plants-International Journal of Phytomedicines and Related Industries 5(3) (2013) 150-154.
[53] G.G. Mohamed, E.M. Zayed, A.M. Hindy, Coordination behavior of new bis Schiff base ligand derived from 2-furan carboxaldehyde and propane-1, 3-diamine. Spectroscopic, thermal, anticancer and antibacterial activity studies, Spectrochimica Acta Part A: Molecular and Biomolecular Spectroscopy 145 (2015) 76-84.
[54] H. Boulebd, Comparative study of the radical scavenging behavior of ascorbic acid, BHT, BHA and Trolox: experimental and theoretical study, Journal of Molecular Structure 1201 (2020) 127210.
[55] C. Liu, L. Zhou, W. Huang, M. Wang, Y. Gu, Synthesis of Furans and Pyrroles from 2-Alkoxy-2, 3-dihydrofurans Through a Nucleophilic Substitution-Triggered Heteroaromatization, Advanced Synthesis & Catalysis 358(6) (2016) 900-918.
[56] L.J. Michelini, W.F. Vaz, L.F. Naves, C.N. Pérez, H.B. Napolitano, Synthesis, Characterization and Conformational Analysis of Two Novel 4 (1H)‐Quinolinones, Journal of the Brazilian Chemical Society 31 (2020) 66-78.
[57] H. Zhang, H. Lu, K. Huang, J. Li, F. Wei, A. Liu, K. Chingin, H. Chen, Selective detection of phospholipids in human blood plasma and single cells for cancer differentiation using dispersed solid-phase microextraction combined with extractive electrospray ionization mass spectrometry, Analyst 145(22) (2020) 7330-7339.
[58] M. Chrzanowska, A. Katafias, A. Kozakiewicz, R. Puchta, R. Van Eldik, Systematic tuning of the reactivity of [RuII (terpy)(N^ N) Cl] Cl complexes, Journal of Coordination Chemistry 71(11-13) (2018) 1761-1777.
[59] F. Aslam, F. Farooq, M.N. Amin, K. Khan, A. Waheed, A. Akbar, M.F. Javed, R. Alyousef, H. Alabdulijabbar, Applications of gene expression programming for estimating compressive strength of high-strength concrete, Advances in Civil Engineering 2020 (2020).
[60] I. Petrik, Characterization and design of hydrogen bonding interactions in oxygen reduction by engineered myoglobins, University of Illinois at Urbana-Champaign, 2016.

دراسة متراكبات جديدة بالتحضير والقياسات الطيفية وبرنامج الجاوسين ودراسة الدوكن والتركيب الجزئ.

إيهاب مصطفى زايد 1

1- قسم الكيمياء الخضراء - المركز القومى للبحوث

تم استخدام التقنيات التحليلية ، الطيف (IR و 1 H NMR) ، الموصلية المولية ، وقياسات العزم المغناطيسية لتجميع وتحليل الترابط (H2L) ومتراكباته. تم دراسة تقنية التحليل الحراري (TG) في درجات حرارة تتراوح من درجة حرارة محيطة إلى 1000 درجة مئوية. يستخدم (H2L) مقترنًا بأيونات المعدن من خلال ذرتين من النيتروجين واثنين من ذرات الأكسجين في وضع سلبي ، وفقًا لأطياف الأشعة تحت الحمراء. تم تقدير فجوات الطاقة والمعايير النظرية الهامة الأخرى باستخدام طريقة DFT / B3LYP ، وتم تحسين الصيغة الهيكلية للرابط المركب باستخدام برنامج Gaussian09. تم استخدام طريقة الأجار لفحص النشاط البيولوجي في المختبر لليجند (H2L) و ومركباته المعدنية ضد بكتيريا الجرام (+) (Bacillus subtilis و Staphylococcus aureus) وبكتيريا الجرام (-) (Escherichia coli و Pseudomonas aeruginosa). أظهرت النتائج أن المجمعات المنتجة أكثر نشاطًا من الناحية الفسيولوجية من الليجند. تم إجراء بحث حول الالتحام الجزيئي بين الترابط والتركيبات البلورية لكل من t88-Escherichia coli3 و ty7-Staphylococcus aureus3 و h67-Bacillus subtilis5 و i39-Pseudomonas aeruginosa5